AIP | APL Materials

Transparent conducting properties of SrSnO3 and ZnSnO3

Khuong P. Ong, Xiaofeng Fan, Alaska Subedi, Michael B. Sullivan, and David J. Singh

Citation: APL Mater. **3**, 062505 (2015); doi: 10.1063/1.4919564
View online: http://dx.doi.org/10.1063/1.4919564
View Table of Contents: http://scitation.aip.org/content/aip/journal/aplmater/3/6?ver=pdfcov
Published by the AIP Publishing

APL MATERIALS **3**, 062505 (2015)

Transparent conducting properties of $SrSnO_3$ and $ZnSnO_3$

Khuong P. Ong,[1] Xiaofeng Fan,[2] Alaska Subedi,[3] Michael B. Sullivan,[1] and David J. Singh[4]

[1]*Institute of High Performance Computing, Agency for Science Technology and Research, 1 Fusionopolis Way, 16-16 Connexis, 138632 Singapore*
[2]*College of Materials Science and Engineering, Jilin University, 130012 Changchun, China*
[3]*Max Planck Institute for the Structure and Dynamics of Matter, Hamburg, Germany*
[4]*Materials Science and Technology Division, Oak Ridge National Laboratory, Oak Ridge, Tennessee 37831-6056, USA*

(Received 5 March 2015; accepted 20 April 2015; published online 29 April 2015)

We report optical properties of doped n-type $SrSnO_3$ and $ZnSnO_3$ in relation to potential application as transparent conductors. We find that the orthorhombic distortion of the perovskite structure in $SrSnO_3$ leads to absorption in the visible as the doping level is increased. This arises from interband transitions. We find that strain tuning could modify this absorption, but does not eliminate it. On the other hand, we find that $ZnSnO_3$ although also having a non-cubic structure, can retain excellent transparency when doped, making it a good candidate transparent conductor. [http://dx.doi.org/10.1063/1.4919564]

Transparent conductors are materials with DC electrical conductivity but transparency to light over a wavelength range of interest. These materials are important in solar photovoltaics, displays, and other technologies. The most commonly used material is the n-type oxide, In_2O_3 doped with Sn (ITO). This material has excellent performance. However, there is an interest in finding alternative materials. This is both because of cost issues associated with a material having a large concentration of In and because of interest in finding materials with higher performance or different properties that may be enabling for new technologies. For example, it would be desirable to find p-type materials that could be used in transparent electronics, materials that operate in different wavelength ranges, or materials that have different mechanical properties and materials compatible with different active electronic materials, e.g., organic or oxide electronics.[1–5] Recently, several new materials have been proposed, one of which is n-type cubic perovskite $BaSnO_3$. This material has a number of advantages. These include the fact that it is In free.[6–12] Here, we investigate the related compounds, n-type $SrSnO_3$ and $ZnSnO_3$, which have smaller lattice parameters, more compatible with common oxide electronic substrates.

We find that in spite of the larger band gap compared to $BaSnO_3$, $SrSnO_3$ will have absorption in the visible when heavily n-type doped, while $ZnSnO_3$ is much more promising. This absorption in $SrSnO_3$ is due to interband transitions from carriers near the conduction band minimum to higher conduction bands and is a consequence of the *Pnma* zone folding and symmetry lowering from cubic. We find that this could be mitigated by epitaxy or alloying that makes the structure cubic or at least changes the tilt pattern to an *M*-point pattern. $ZnSnO_3$, which has a rhombohedral *R*-point derived, $LiNbO_3$ ferroelectric structure that combines tilts and large *A*-site displacements,[13] is predicted to retain visible light transparency when heavily doped and has favorable electronic properties as well. Therefore, $ZnSnO_3$ may be expected to be a particularly good transparent conductor when doped n-type. A challenge will be the development of high mobility films for this strongly non-cubic material.

A guiding principle for bulk compounds is that a transparent conductor should have a suitably large band gap, i.e., above 3.25 eV for visible light application and should be amenable to heavy doping to obtain conductivity. However, while there are many materials that can be doped and have band gaps above 3.25 eV, there are only a handful of known useful high performance transparent

conductors. In this regard, limitations beyond band gap and dopability need to be considered. These include additional absorption in heavily doped materials both from the Drude tail[14–16] and from interband transitions involving the doped carriers.[17] The former gives absorption primarily in the infrared and red, while the latter can be at any wavelength and depends on the details of the band structure.

Within the Drude model, $\sigma(\omega) = \sigma_0/(1 + i\omega\tau)$, where τ is an inverse scattering rate and σ_0 is the DC conductivity, $\sigma_0 = \omega_p^2\tau$. Here, ω_p is the plasma frequency. The square of the plasma frequency is ne^2/m for a parabolic band with effective mass m and carrier concentration n and is an integral of the squared band velocity over the Fermi surface in a general case. $\Omega_p = \hbar\omega_p$ is used here as the plasma energy. High DC conductivity requires a combination of weak scattering and high plasma frequency, while for a given ω_p, the Drude tail in the red is reduced if the scattering rate can be lowered. This favors materials with simple band structures, weak electron-electron scattering, absence of magnetism, weak electron-phonon interactions, and good screening (i.e., high dielectric constant). Kioupakis and co-workers have presented a detailed analysis and first principles calculations of these effects in group-III nitrides.[18]

As mentioned, $BaSnO_3$ shows considerable promise as a new n-type transparent conducting oxide (TCO). This material, which has a simple *s*-band electronic structure,[17,19–24] is dopable to a highly conductive state using Sb or La,[25] and has been developed as a high performance TCO.[6–12] The related compounds, $CaSnO_3$ and $SrSnO_3$, occur in distorted orthorhombic perovskite structures,[26] while $ZnSnO_3$ occurs in a ferroelectric $LiNbO_3$ type structure.[13,27–30] Amorphous zinc-tin-oxide amorphous films were already been successfully developed for transparent electronics ten years ago,[31] while mixed phase films with compositions near $ZnSnO_3$ are known to show good TCO properties.[32,33] Nonetheless, indium containing amorphous In-Ga-Zn-O (IGZO) films is dominant in technological applications of transparent amorphous oxide electronics due to their performance.[3,34] Single phase films of spinel structure Zn_2SnO_4, known as ZTO, also show promising TCO properties.[35] These zinc-tin-oxide films show a number of advantages, including chemical stability and relatively facile growth of high quality films. In any case, $BaSnO_3$, $SrSnO_3$, and $ZnSnO_3$ all have Sn *s* derived conduction bands, suggesting that they might all be good transparent conductors. In fact, the lattice parameter of $SrSnO_3$ is better lattice matched to technologically interesting substrates, such as $SrTiO_3$ and it has a higher band gap than $BaSnO_3$ suggesting that it might be a very interesting TCO. $ZnSnO_3$ is ferroelectric, and therefore it and modifications of it may be expected to have high mobility when doped due to the high dielectric constants.[36]

In general, scattering in doped non-magnetic oxide films can come from point defects, extended defects (dislocations, grain boundaries, etc.), and intrinsic electron-electron and electron-phonon scattering. Electron-electron scattering is generally insignificant at room temperature for simple non-magnetic oxides and in principle at least grain boundaries, dislocations and most point defects can be regarded as controllable. This leaves electron-phonon interactions as the limiting factor for the best performance that can be achieved in a given material. Electron-phonon scattering in general will give strongest absorption in the red. Heavily doped TCO films will have a resistivity that increases approximately linearly with temperature, and at least increasing with temperature, in this electron-phonon limited, degenerately doped case.[37] However, based on published data, current $BaSnO_3$ films while having promising performance, have not yet reached this limiting behavior, indicating that further improvement is possible. Infrared measurements of phonon frequencies for $BaSnO_3$ have been reported,[38] along with several calculations.[22,23,39] In comparing the three materials, $BaSnO_3$, $SrSnO_3$, and $ZnSnO_3$, another effect of phonons may also be important. Specifically, high dielectric constants can lead to higher mobility due to screening of defects. This may be particularly favorable for $ZnSnO_3$, which when undoped is a ferroelectric.[13]

The present electronic structure and optical calculations were done using the general potential linearized augmented planewave (LAPW) method,[40] as implemented in the WIEN2k code.[41] The results from the optical calculations (see below) motivated structural studies of $SrSnO_3$. We tested various sets of LAPW sphere radii. The electronic structure results presented are with LAPW sphere radii of 2.4 bohrs, 2.25 bohrs, and 1.55 bohrs for Sr, Sn, and O, respectively, in $SrSnO_3$ and 2.2 bohrs, 2.2 bohrs, and 1.55 bohrs, for Zn, Sn, and O, respectively, in $ZnSnO_3$. The calculations were based on the experimental lattice parameters for both materials. The internal coordinates were

relaxed via energy minimization with the generalized gradient approximation of Perdew, Burke, and Ernzerhof (PBE-GGA).[42] The lattice parameters used were a = 5.5622 Å, c = 14.0026 Å, for $R3c$ (hexagonal setting) $ZnSnO_3$,[13] and a = 5.703 40 Å, b = 8.064 82 Å, c = 5.708 92 Å, for *Pnma* $SrSnO_3$.[43] By comparison, the lattice parameter of cubic $BaSnO_3$ is a = 4.116 Å. This is poorly matched to standard perovskite oxide substrates and is a challenge for development of this material.

For the study of the structure under epitaxial strain, we did calculations with both the PBE-GGA and with the modification of it optimized for solids (PBE-SOL).[44] These two functionals gave similar results. The electronic structure and optical properties were calculated with the optimized atomic positions. We used the modified Becke-Johnson potential functional of Tran and Blaha (TB-mBJ) for these properties.[45] This functional gives greatly improved band gaps for simple insulators and semiconductors when compared to conventional semilocal density functionals.[45–49] The TB-mBJ functional gives good agreement with experimental band gaps for simple oxides, including ferroelectric transition metal oxides such as $Bi_4Ti_3O_{12}$,[50] but does not correctly treat correlated oxides, such as antiferromagnetic Mott insulators.[48,49] Doping was treated keeping the crystal structure fixed and employing the virtual crystal approximation (VCA), which is an average potential approximation. For $SrSnO_3$, we used the Sr site for doping, while in $ZnSnO_3$, we did calculations for doping on each of the three sites. As discussed below, the results with doping on the different sites were very similar. The fact that the site dependence is weak means that the average potential approximation implicit in the virtual crystal approximation is likely to be good, and additionally that doping on the different sites is likely to be possible. Specifically, it means that besides doping with trivalents on the Zn site (e.g., Ga, In, Y, etc.), one could obtain conductivity by doping on the Sn site, e.g., with Sb or on the O site, e.g., with F. It also means that co-doping by a combination of these may be useful in increasing the doping range without destroying the mobility.

Our calculated TB-mBJ band gaps are 3.70 eV for orthorhombic $SrSnO_3$ and 3.05 eV for ferroelectric $ZnSnO_3$. We also considered $SrSnO_3$ in a cubic structure with the same volume as the experimental structure as well as with constrained structures having octahedral rotations of 10° about the c-axis with M- and R-point ordering. The spacegroups are $SrSnO_3$ experimental, *Pnma*, no. 62; cubic, $Pm\bar{3}m$, no. 221; M-point, $P4/mbm$, no. 127; R-point, $I4/mcm$, no. 140; and $ZnSnO_3$, experimental, $R3c$, no. 161. Note, however that the M-point structure is a disfavored perovskite structure that is not normally observed (repulsion between O ions generally favors R-point or a more complex combination of tilts). The band gaps for these structures, denoted, cubic, R, and M in the following were 3.63 eV, 3.62 eV, and 3.68 eV, respectively. The relatively weak dependence of the gap on octahedral tilt at fixed volume is consistent with results of Ref. 24. In all cases, the conduction band minimum (CBM) is formed by a Sn s derived band and the gaps were indirect. The band structures are shown in Fig. 1. The band structure of ferroelectric $ZnSnO_3$ is shown in Fig. 2. The calculated band gap of $BaSnO_3$ by the same method is 2.82 eV and is indirect, with an onset of optical absorption from direct transitions at ~3.2 eV,[17,24] in excellent accord with experimental data.[12]

Band structures of $ZnSnO_3$ using standard GGA functionals have been reported by Wang and co-workers[51] and by Zhang and co-workers.[30] These show lower band gaps, but otherwise similar band shapes.

The singly degenerate Γ-point conduction band minimum of orthorhombic *Pnma* $SrSnO_3$ is characterized by a diagonal effective mass tensor, with calculated components, $m_a = 0.38m_e$, $m_b = 0.42m_e$ and $m_c = 0.43m_e$. The conduction band minimum of $ZnSnO_3$, also at the zone center, has calculated $m_{ab} = 0.32m_e$ and $m_c = 0.32m_e$. For comparison, the calculated conduction band minimum effective mass of cubic $BaSnO_3$ by the same method is $0.26m_e$. All of these are small enough to be consistent with high conductivity when doped n-type.

The conduction band structure of cubic $SrSnO_3$ is qualitatively similar to that of $BaSnO_3$ (see Ref. 21). In cubic $SrSnO_3$, the gap between the CBM and the next conduction band at Γ is 3.2 eV. This is reduced to 2.9 eV in the actual *Pnma* structure. This means that depending on matrix elements, absorption in the visible due to transitions from the lowest conduction band may be anticipated when doped. This gap is larger for the R-point and M-point distorted structures at 3.6 eV in both cases. This means that for both M- and R-point distortions as well as cubic, one would have some n-type doping range before interband absorption starts, but this range will be limited since the

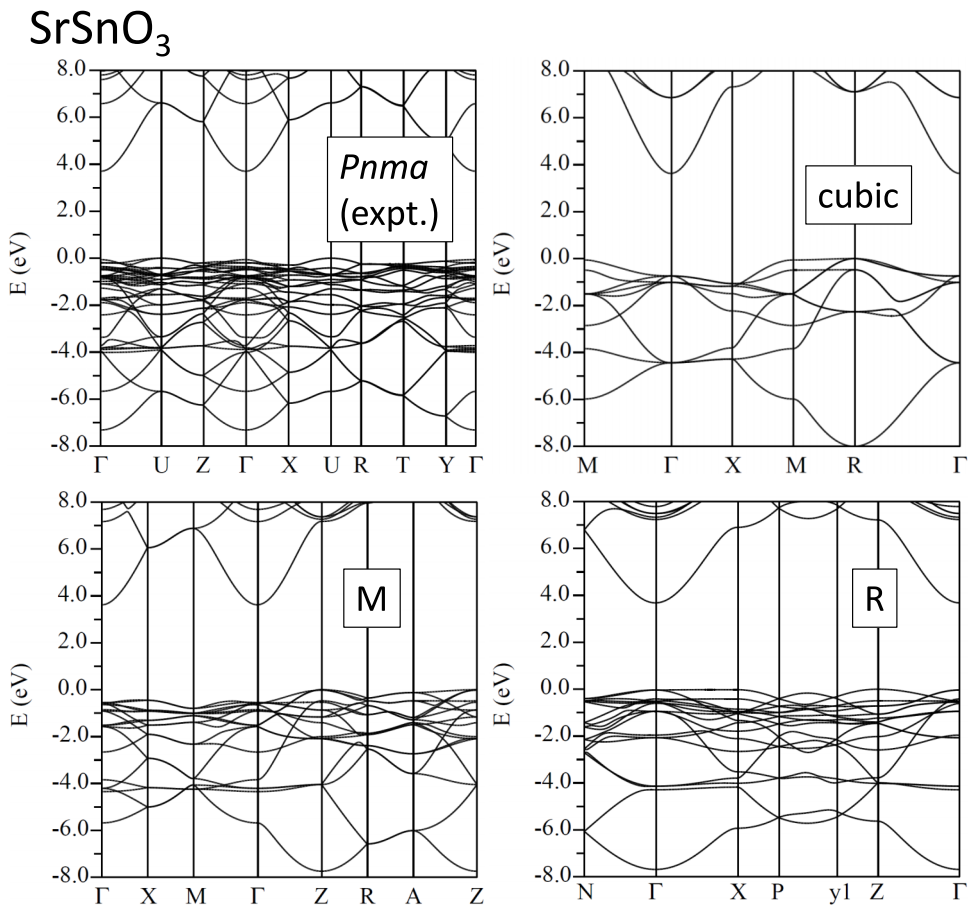

FIG. 1. Calculated band structures of $SrSnO_3$ in its experimental *Pnma* structure and iso-volume cubic, M and R structures (see text).

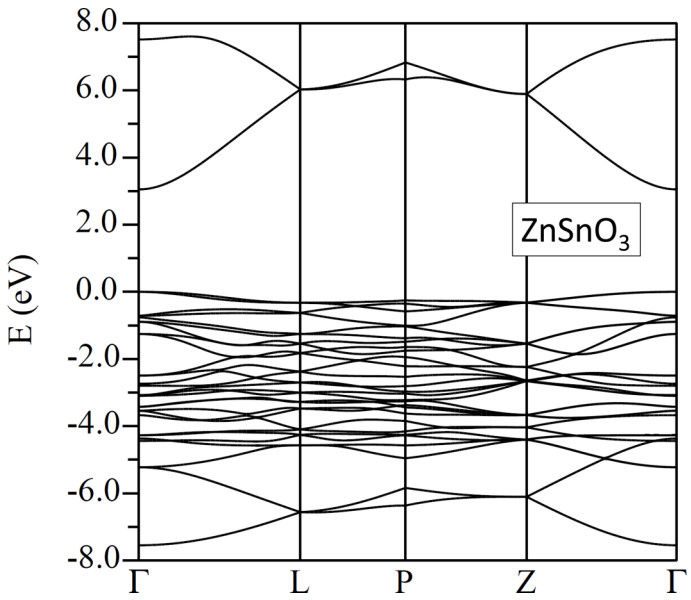

FIG. 2. Calculated band structure of ferroelectric $ZnSnO_3$.

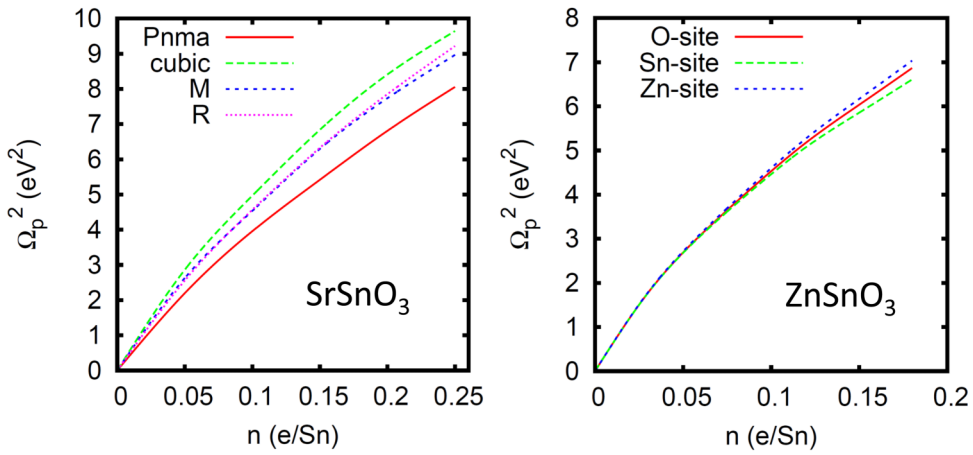

FIG. 3. Calculated direction averaged squared plasma energies for $SrSnO_3$ virtual crystal doped on the Sr site (left) in its experimental *Pnma* structure and iso-volume cubic, *R*- and *M*-structures (see text), and $ZnSnO_3$ with different doping sites crystal doped (on the Sr site) $SrSnO_3$ (left) in its experimental *Pnma* structure and iso-volume cubic, M and R structures and $ZnSnO_3$ (right) with virtual crystal doping on the different sites.

Fermi level will increase with doping level. The light bands, which are what favors good mobility, also mean that this rise is significant. For a doping level of 0.15 e/Sn, we obtain a Fermi level that is 1.3 eV above the CBM. The value 0.15 e/Sn is a high but achievable value for $BaSnO_3$. Thin film samples doped with La generally have a lower La content, while work on Sb doped samples show increasing conductivity up to Sb contents of 0.15, which corresponds to this doping level.[25]

As mentioned, the conductivity of a metal or degenerately doped semiconductor is related to the plasma frequency by $\sigma_0 = \omega_p^2 \tau$. Fig. 3 shows the calculated plasma energies as a function of doping for the two compounds. These were obtained by direct integration over the Fermi surface using the optical package of WIEN2k. As seen, the behaviors of $ZnSnO_3$ and $SrSnO_3$ are similar; the virtual crystal approximation is supported by the similarity of the results for doping on different sites for $ZnSnO_3$ and while there is some variation with structure in $SrSnO_3$, it is minor. From this point of view, both compounds are reasonable TCO candidates, reflecting the Sn *s* character of the lowest conduction bands. However, conductivity when doped is only part of the requirement for a TCO.

Fig. 4 shows the calculated absorption due to interband transitions (i.e., not including Drude absorption, which would be additional), for a heavy doping of 0.15 e/Sn. As shown, there is significant interband absorption in the visible for $SrSnO_3$ in its experimental structure. This is from direct vertical transitions. In addition, there will generally be phonon assisted (non-vertical) transitions that contribute to absorption, but these would be much weaker than direct transitions when direct transitions are allowed. In any case, this interband absorption will increase in magnitude and come into the visible from the blue side as the compound is increasingly doped n-type. This absorption persists for the *R*-point structure but is largely removed for both the cubic and *M*-point structures. Thus, octahedral tilts in the experimental structure of $SrSnO_3$ lead to absorption in the visible, which is detrimental in a TCO. The magnitude of the absorption (Fig. 4) is not so large as to mean that $SrSnO_3$ could not be used as a TCO, but it does mean that intrinsically $SrSnO_3$ is expected to be inferior to optimized $BaSnO_3$. Octahedral tilts in perovskites can often by suppressed by alloying with larger A-site cations, e.g., replacing Sr by Ba, but this strategy for improving $SrSnO_3$ by going to $BaSnO_3$ defeats the purpose of examining $SrSnO_3$.

Tensile strain is another general way of reducing tilt instabilities, but considering the lattice parameters of $SrSnO_3$ in relation to technological substrates and because the band gap decreases strongly with tensile strain,[24] we decided to focus on compression here to see if $SrSnO_3$ might be a useful TCO on substrates with smaller lattice parameters. This was done by calculating relaxed structures with 2D epitaxial strain as a function of strain. We considered a number of different plausible structures (see Ref. 52 for a description), as indicated in Fig. 5. We find that at sizable, but

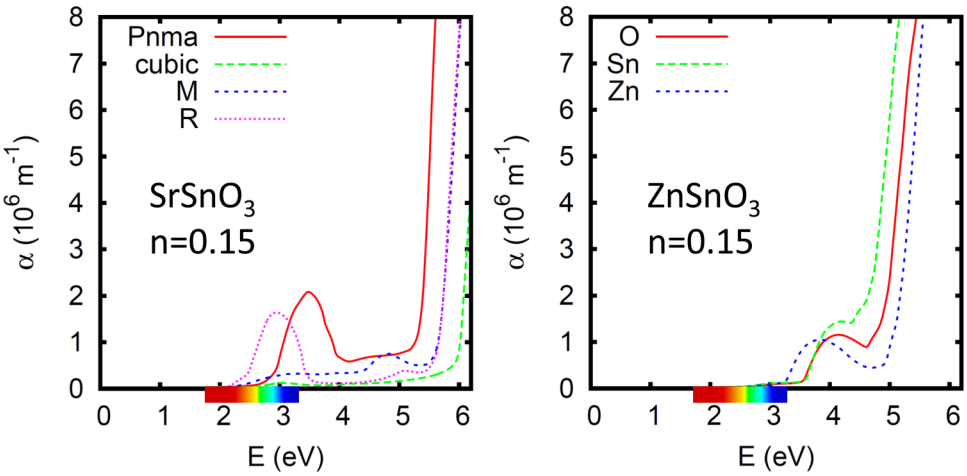

FIG. 4. Calculated direction averaged absorption spectra for virtual crystal doped (on the Sr site) $SrSnO_3$ (left) in its experimental *Pnma* structure and iso-volume cubic, *M*- and *R*-structures, and $ZnSnO_3$ (right) with virtual crystal doping on the different sites. The color bars on the horizontal axes approximately indicate the visible, 1.7 eV–3.25 eV.

potentially achievable, compressive strains of ~2%–3% are needed to produce a change in structure, and that among the structures, we investigated the lowest energy structure at high compression is the *R*-point structure, space group $I4/mcm$, which also suffers from absorption in the visible at high doping. Thus, we conclude that $SrSnO_3$ will be generally a more difficult material to use as a TCO than $BaSnO_3$.

$ZnSnO_3$ on the other hand shows very favorable behavior when doped, both from the point of view of the plasma frequency and from the absence of interband absorption when heavily doped. This is in spite of its highly distorted $LiNbO_3$ type structure. Furthermore, we note that $ZnSnO_3$ is a ferroelectric material. While ferroelectricity as strictly defined is incompatible with metallic conduction, we note that semiconductors with high dielectric constants are generally expected to have high mobility due to screening of impurities and other defects.[36,53] This plus the high plasma

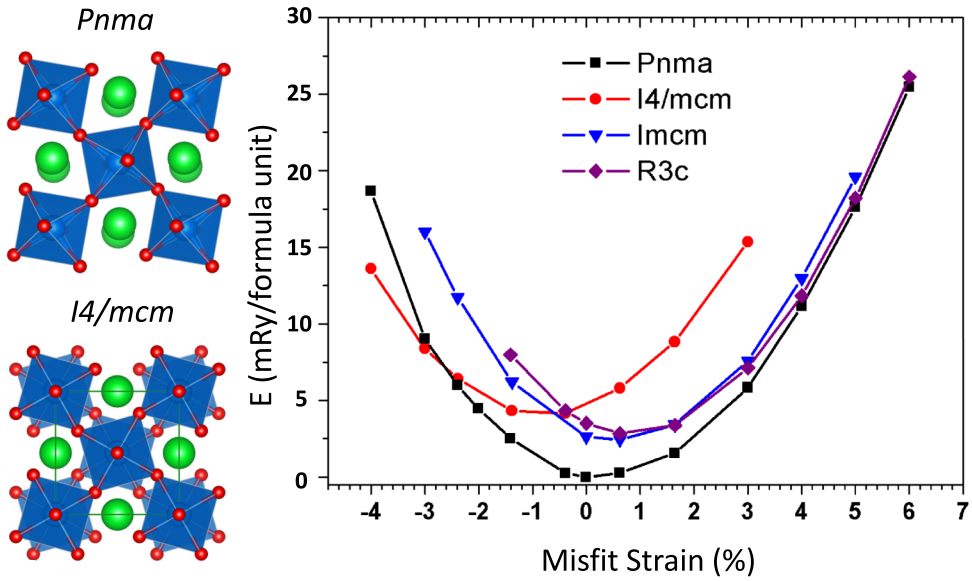

FIG. 5. Evolution of the structure of $SrSnO_3$ under (001) compressive epitaxial strain (right) and a depiction of the two low energy structures (left), i.e., the experimental ambient structure (Pnma) and the *R*-structure. In this plot, the PBE-SOL GGA was used, and the 0 strain level is at the calculated effective lattice parameter of 4.037 Å.

frequencies when doped indicate the potential for high mobility. The evolution of the properties of $ZnSnO_3$ relevant to TCO behavior is much more similar to that of $BaSnO_3$ than what is found for $SrSnO_3$. In any case, the present results indicate that n-type doped crystalline $LiNbO_3$ structure, $ZnSnO_3$, is likely to be a very high performance TCO comparable to $BaSnO_3$.

To conclude, we find that n-type doped $SrSnO_3$ could potentially be used as a TCO, and because of its higher band gap it might be useful in applications where some transparency in the near ultraviolet is desired. However, its intrinsic performance for visible light at high doping levels is expected to be inferior to optimized $BaSnO_3$. On the other hand, the results indicate that n-type crystalline $LiNbO_3$ structure $ZnSnO_3$ is very promising as a high performance TCO material. We note, however, that to date high mobility $ZnSnO_3$ films with this structure have not been reported. One challenge will be the growth of films with low densities of grain and domain boundaries, which may limit conductivity in this distorted ferroelectric material. Nonetheless, the present results suggest investigation of this material and its doping.

Work at ORNL was supported by the Department of Energy, Office of Science, Basic Energy Sciences, Materials Sciences and Engineering Division. Work at IHPC was supported by the Singapore Agency for Science Technology and Research (A*STAR). We are grateful for useful discussions with Bharat Jalan.

[1] D. S. Ginley and C. Bright, MRS Bull. **25**, 15 (2000).
[2] H. Kawazoe, H. Yanagi, K. Ueda, and H. Hosono, MRS Bull. **25**, 28 (2000).
[3] K. Nomura, H. Ohta, A. Takagi, T. Kamiya, M. Hirano, and H. Hosono, Nature (London) **432**, 488 (2004).
[4] X. Wang, L. Zhi, and K. Mullen, Nano Lett. **8**, 323 (2008).
[5] J. Y. Lee, S. T. Connor, Y. Cui, and P. Peumans, Nano Lett. **8**, 689 (2008).
[6] H. Mun, U. Kim, H. M. Kim, C. Park, T. H. Kim, H. J. Kim, K. H. Kim, and K. Char, Appl. Phys. Lett. **102**, 252105 (2013).
[7] H. J. Kim, U. Kim, H. M. Kim, T. H. Kim, H. S. Mun, B. G. Jeon, K. T. Hong, W. J. Lee, C. Ju, K. H. Kim, and K. Char, Appl. Phys. Express **5**, 061102 (2012).
[8] H. Mizoguchi, P. Chen, P. Boolchand, V. Ksenofontov, C. Felser, P. W. Barnes, and P. M. Woodward, Chem. Mater. **25**, 3858 (2013).
[9] S. Upadhyay, O. Parkash, and D. Kumar, J. Phys. D: Appl. Phys. **37**, 1483 (2004).
[10] P. V. Wadekar, J. Alaria, M. O'Sullivan, N. L. O. Flack, T. D. Manning, L. J. Phillips, K. Durose, O. Lozano, S. Lucas, J. B. Claridge, and M. J. Rosseinsky, Appl. Phys. Lett. **105**, 052104 (2014).
[11] S. Sallis, D. O. Scanlon, S. C. Chae, N. F. Quackenbush, D. A. Fischer, J. C. Woicik, J. H. Guo, S. W. Cheong, and L. F. J. Piper, Appl. Phys. Lett. **103**, 042105 (2013).
[12] H. J. Kim, U. Kim, T. H. Kim, J. Kim, H. M. Kim, B.-G. Jeon, W.-J. Lee, H. S. Mun, K. T. Hong, J. Yu, K. Char, and K. H. Kim, Phys. Rev. B **86**, 165205 (2012).
[13] Y. Inaguma, M. Yoshida, and T. Katsumata, J. Am. Chem. Soc. **130**, 6704 (2008).
[14] I. Hamberg and C. G. Granqist, J. Appl. Phys. **60**, R123 (1986).
[15] A. Porch, D. V. Morgan, R. M. Perks, M. O. Jones, and P. P. Edwards, J. Appl. Phys. **95**, 4734 (2004).
[16] A. J. Freeman, K. R. Poeppelmeier, T. O. Mason, R. P. H. Chang, and T. J. Marks, MRS Bull. **25**, 45 (2000).
[17] Y. Li, L. Zhang, Y. Ma, and D. J. Singh, APL Mater. **3**, 011102 (2015).
[18] E. Kioupakis, P. Rinke, A. Schleife, F. Bechstedt, and C. G. Van de Walle, Phys. Rev. B **81**, 241201 (2010).
[19] D. J. Singh, D. A. Papaconstantopoulos, J. P. Julien, and F. Cyrot-Lackmann, Phys. Rev. B **44**, 9519 (1991).
[20] H. Mizoguchi, H. W. Eng, and P. M. Woodward, Inorg. Chem. **43**, 1667 (2004).
[21] X. F. Fan, W. T. Zheng, X. Chen, and D. J. Singh, PLoS One **9**, e91423 (2014).
[22] B. G. Kim, J. Y. Jo, and S. W. Cheong, J. Solid State Chem. **197**, 134 (2013).
[23] H. R. Liu, J. H. Yang, H. J. Xiang, and S. H. Wei, Appl. Phys. Lett. **102**, 112109 (2013).
[24] D. J. Singh, Q. Xu, and K. P. Ong, Appl. Phys. Lett. **104**, 011910 (2014).
[25] R. J. Cava, P. Gammel, B. Batlogg, J. J. Krajewski, and W. F. Peck, Jr., Phys. Rev. B **42**, 4815 (1990).
[26] A. Vegas, M. Vallet-Regi, J. M. Gonzalez-Calbet, and M. A. Alario-Franco, Acta Crystallogr., Sect. B: Struct. Sci. **42**, 167 (1986).
[27] D. Kovacheva and K. Petrov, Solid State Ionics **109**, 327 (1998).
[28] M. Nakayama, M. Nogami, M. Yoshida, T. Katsumata, and Y. Inaguma, Adv. Mater. **22**, 2579 (2010).
[29] J. Y. Son, G. Lee, M. H. Jo, H. Kim, H. M. Jang, and Y. H. Shin, J. Am. Chem. Soc. **131**, 8386 (2009).
[30] J. Zhang, K. L. Yao, Z. L. Liu, G. Y. Gao, Z. Y. Sun, and S. W. Fan, Phys. Chem. Chem. Phys. **12**, 9197 (2010).
[31] H. Q. Chiang, J. F. Wager, R. L. Hoffman, J. Jeong, and D. A. Keszler, Appl. Phys. Lett. **86**, 013503 (2005).
[32] T. Minami, S. Takata, H. Sato, and H. Sonohara, J. Vac. Sci. Technol., A **13**, 1095 (1995).
[33] T. Minami, H. Sonohara, S. Takata, and H. Sato, Jpn. J. Appl. Phys., Part 2 **33**, L1693 (1994).
[34] T. Kamiya, K. Nomura, and H. Hosono, Sci. Technol. Adv. Mater. **11**, 044305 (2010).
[35] D. L. Young, H. Moutinho, Y. Yan, and T. J. Coutts, J. Appl. Phys. **92**, 310 (2002).
[36] M. H. Du and D. J. Singh, Phys. Rev. B **81**, 144114 (2010).
[37] P. B. Allen, Phys. Rev. B **36**, 2920 (1987).
[38] T. N. Stanislavchuk, A. A. Sirenko, A. P. Litvinchuk, X. Luo, and S. W. Cheong, J. Appl. Phys. **112**, 044108 (2012).
[39] E. Bevillon, A. Chesnaud, Y. Wang, G. Dezanneau, and G. Geneste, J. Phys.:Condens. Matter **20**, 145217 (2008).
[40] D. J. Singh and L. Nordstrom, *Planewaves Pseudopotentials and the LAPW Method*, 2nd ed. (Springer, Berlin, 2006).

[41] P. Blaha, K. Schwarz, G. Madsen, D. Kvasnicka, and J. Luitz, WIEN2k, An Augmented Plane Wave + Local Orbitals Program for Calculating Crystal Properties Karlheinz Schwarz, Tech. Univ., Wien, Austria, (2001).
[42] J. P. Perdew, K. Burke, and M. Ernzerhof, Phys. Rev. Lett. **77**, 3865 (1996).
[43] M. A. Green, K. Prassides, P. Day, and D. A. Neumann, J. Chem. Soc., Faraday Trans. **92**, 2155 (1996).
[44] J. P. Perdew, A. Ruzsinszky, G. I. Csonka, O. A. Vydrov, G. E. Scuseria, L. A. Constantin, X. Zhou, and K. Burke, Phys. Rev. Lett. **100**, 136406 (2008).
[45] F. Tran and P. Blaha, Phys. Rev. Lett. **102**, 226401 (2009).
[46] D. J. Singh, Phys. Rev. B **82**, 155145 (2010).
[47] D. Koller, F. Tran, and P. Blaha, Phys. Rev. B **83**, 195134 (2011).
[48] D. J. Singh, Phys. Rev. B **82**, 205102 (2010).
[49] Y. S. Kim, M. Marsman, G. Kresse, F. Tran, and P. Blaha, Phys. Rev. B **82**, 205212 (2010).
[50] D. J. Singh, S. S. A. Seo, and H. N. Lee, Phys. Rev. B **82**, 180103 (2010).
[51] H. Wang, H. Huang, and B. Wang, Solid State Commun. **149**, 1849 (2009).
[52] Z. Fan, J. Wang, M. B. Sullivan, A. Huan, D. J. Singh, and K. P. Ong, Sci. Rep. **4**, 4631 (2014).
[53] W. Siemons, M. A. McGuire, V. R. Cooper, M. D. Biegalski, I. N. Ivanov, G. E. Jellison, Jr., L. A. Boatner, B. C. Sales, and H. M. Christen, Adv. Mater. **24**, 3965 (2012).